Supplementary Information

Figure S1 shows closeup views of the images in Figure 2. Visual observation makes it clear that the fabrication resolution of the CW mode decreases as exposure dose increases. By comparison, the FPP mode can maintain fine resolution even at excessive exposure doses.

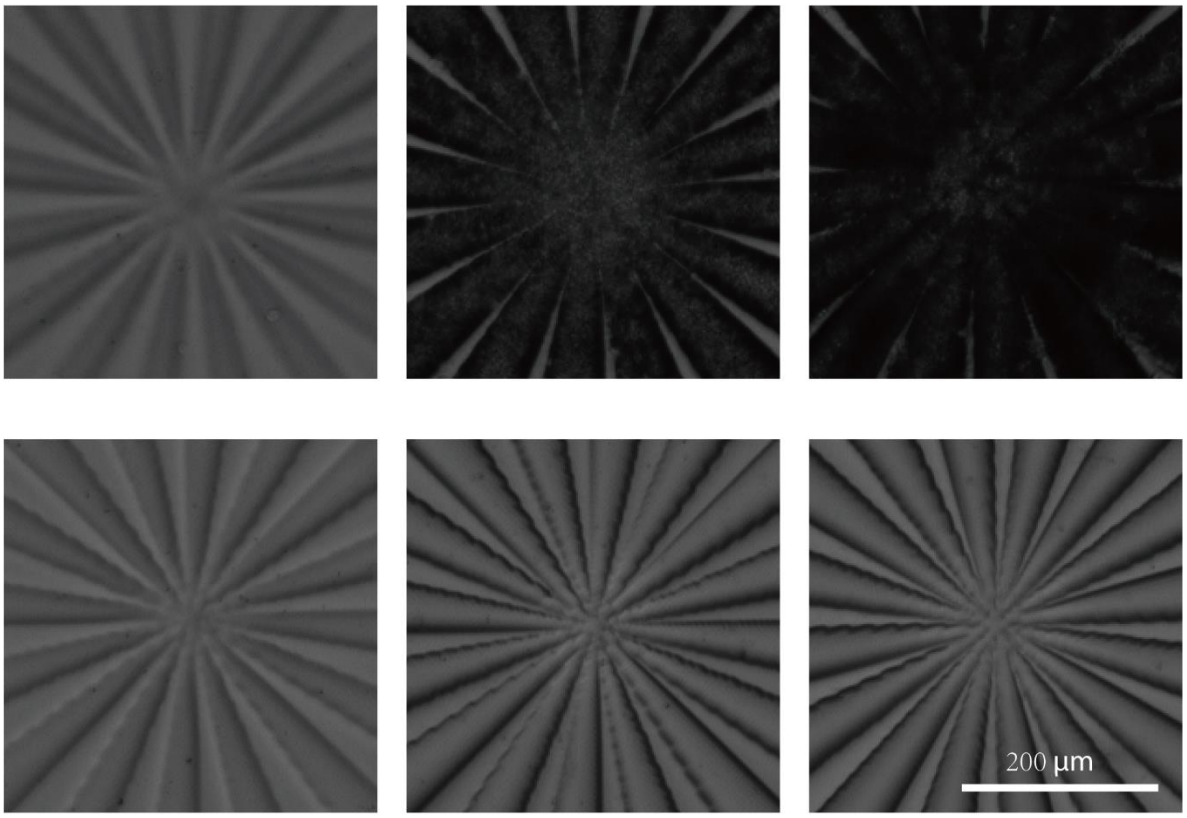

Figure S1. Zoom-in view of images in Figure 2. First row: patterns printed with CW exposure.

Second row: patterns printed with FPP.

The slab samples for scattering measurement in Figure 3 have different visual appearances. The CW sample is much more opaque than the FPP sample. Figure S2 shows the appearance of the two samples.

Journal P

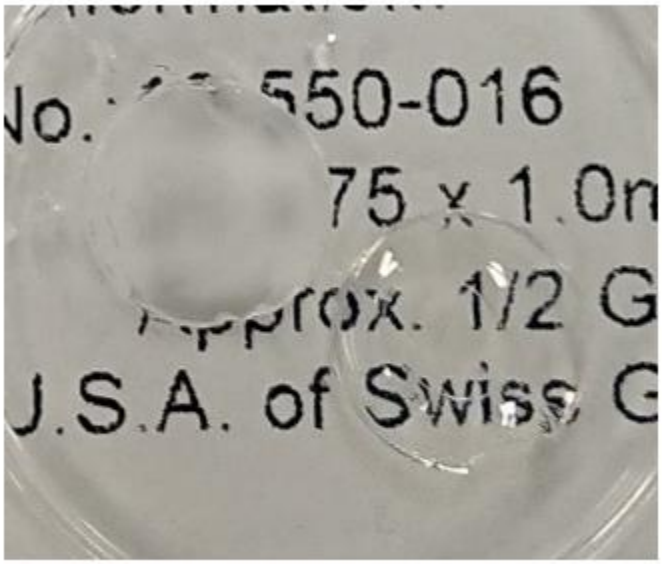

Figure S2. Appearance of the slab samples. The upper-left disc is made by CW exposure, and the lower-right disc is made by FPP exposure

In order to visualize the opacification during photopolymerization in real-time, a high-speed camera was used to record the change of Tyndall effect on a photopolymerizable material. The material is aqueous 50% (v/v) PEGDA with 4% (w/v) LAP added as the photoinitiator. The prepolymer solution was loaded in a cuvette, and a He-Ne laser beam (633 nm) was shone through the solution such that the beam path and its shape was visible to the high-speed camera (Figure S3). Finally, either a UV-LED light source (365 nm) or a xenon flash tube was set up near the cuvette to photopolymerize the PEGDA solution.

The UV-LED was record to have a light intensity of 12 mW cm^{-2} at the cuvette. The xenon flash tube has a broad emission spectrum encompassing from UV to NIR, with an electrical energy per flash of 40 J. However, we did not have a suitable instrument to measure the actual light intensity of the flash illumination at the cuvette. The high-speed camera was set to record at 500 fps, with a 2 ms exposure time for each frame. The image was recorded at monochromatic 16-bit

Journal Pre-proof

bit-depth, and the gray scale value ranged from 0 to 65535. The original recorded grey scale value was used as the intensity in Figure S4 (b) and (d). The beginning and ending time of exposure was determined based on the subtle change of background brightness, since the long pass filter does not completely block the light from the LED or flash tube.

We used either a 2.3-second CW exposure from the UV-LED or a single flashing exposure from the xenon flash tube to polymerize the prepolymer solution. The change of shape of the laser beam inside the PEGDA was recorded, as shown in Figure S4(a) for CW exposure and in Figure S4(c) for FPP exposure. The intensity profiles along the green arrows were plotted in Figure S4(b) for CW exposure and in Figure S4(d) for FPP exposure.

As was expected, light scattering increased during photopolymerization in both cases. In the CW exposure case, scattering steadily increases during the 2.3-second exposure, and at the end of exposure period the material is highly scattering, with scattering still continuing to increase even after the exposure period. In the FPP exposure case, the first 50 milliseconds of the recorded video was strongly interfered with by the intense flashing, and laser beam shape was unable to be observed, but at the end of the flash (t = 50 ms), the material scattering has increased only slightly. The scattering keeps increasing in the next several hundreds of milliseconds.

Journal Pre-proof

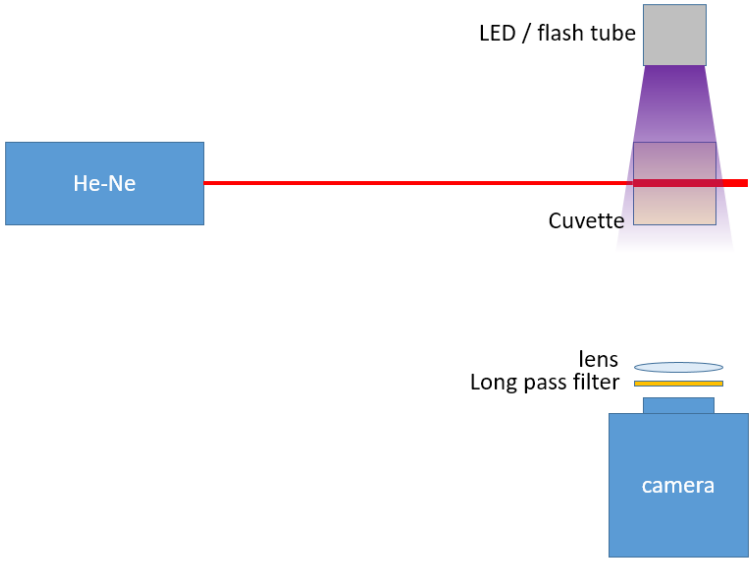

Figure S3. Optical setup for visualizing the opacification during polymerization.

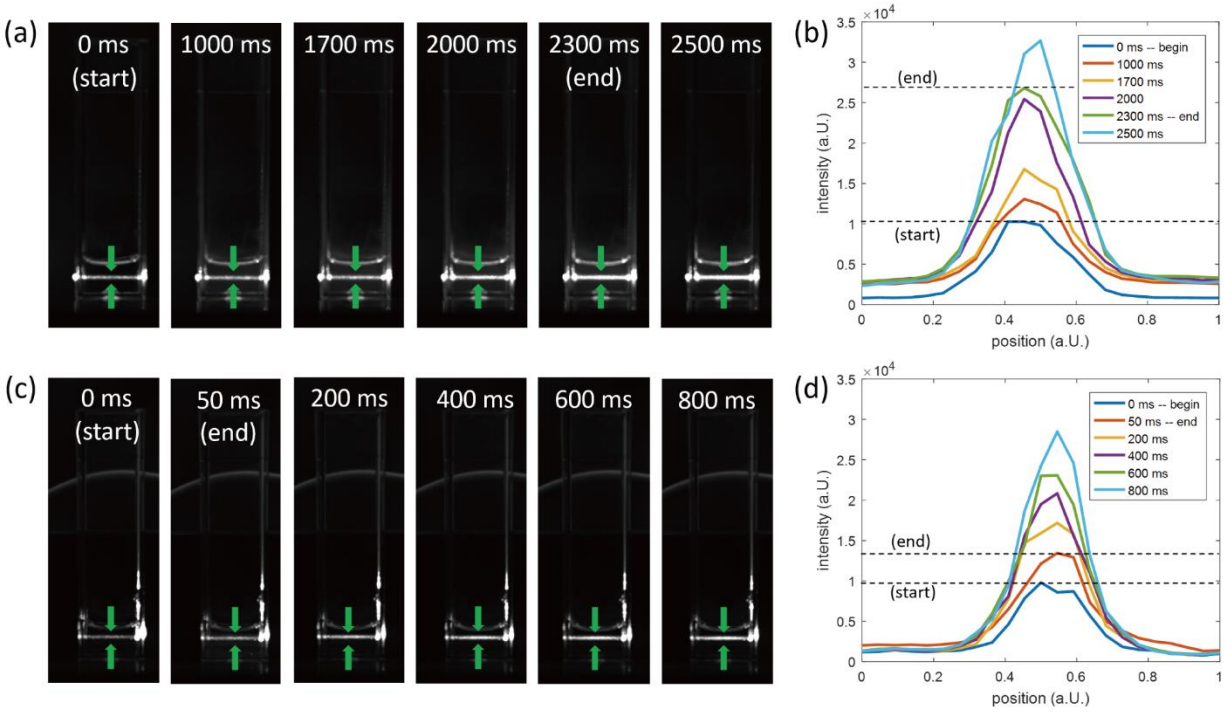

Figure S4. Scattering changes during polymerization. (a) Images of Tyndall effect at different time point of CW exposure. (b) Intensity profile of the laser beam along the green arrows in (a). (c) Images of Tyndall effect at different time points of FPP exposure. (d) Intensity profile of the laser beam along the green arrows in (c).

In the simulation, the type and concentration of photoinitiator, and the illumination intensity are given, thus the free radical generation rate can be calculated, then the kinetics simulation can be performed with Equations (1) – (11). Here is the method to convert the illumination intensity into free-radical generation rate.

The free radical generation rate r_i is proportional to the quantity of photons absorbed per unit time per unit volume N_{abs}, and to the quantum efficiency Φ:

$$r_i = 2\Phi N_{abs} \tag{S1}$$

According to Beer-Lambert law, the molar quantity of photons absorbed, N_{abs} per unit volume is related to the material absorbance A, light power intensity I, sample thickness L, and photon frequency ν:

$$N_{abs} = (1 - 10^{-A}) \cdot \frac{I}{N_A h\nu} \cdot \frac{1}{L} \tag{S2}$$

where N_A and h are Avogadro constant and Plank constant.

The material absorbance A is determined by the molar extinction coefficient ε, the photoinitiator concentration C (neglecting monomer absorption), and the sample thickness L.

$$A = \frac{\varepsilon C L}{\ln(10)} \tag{S3}$$

Combining Equations (S1) – (S3), the free radical generation rates at different illumination intensities can be calculated. Table S1 lists the corresponding free radical generation rates associated with the light illumination intensities used in the simulation.

Journal Pre-proof

Table S1. Free radical generation rates and corresponding illumination intensity.

Free Radical Generation Rate	Light Intensity
0.0005 mol L^{-1} s^{-1}	1.1 mW cm^{-2}
0.001 mol L^{-1} s^{-1}	2.2 mW cm^{-2}
0.002 mol L^{-1} s^{-1}	4.3 mW cm^{-2}
50 mol L^{-1} s^{-1}	106.5 W cm^{-2}
55 mol L^{-1} s^{-1}	117.2 W cm^{-2}
60 mol L^{-1} s^{-1}	127.8 W cm^{-2}

Journal Pre-proof